

State resolved photofragmentation of Ni(CO)₄ at 193, 248, and 308 nm: A detailed study of the photodissociation dynamics

F. J. Schlenker, F. Bouchard, I. M. Waller, and J. W. Hepburn

Citation: *The Journal of Chemical Physics* **93**, 7110 (1990); doi: 10.1063/1.459434

View online: <http://dx.doi.org/10.1063/1.459434>

View Table of Contents: <http://scitation.aip.org/content/aip/journal/jcp/93/10?ver=pdfcov>

Published by the [AIP Publishing](#)

Articles you may be interested in

[Photodissociation dynamics of enolic-acetylacetone at 266, 248, and 193 nm: Mechanism and nascent state product distribution of OH](#)

J. Chem. Phys. **118**, 2590 (2003); 10.1063/1.1535424

[Photodissociation dynamics of carbon suboxide at 193 and 248 nm](#)

J. Chem. Phys. **94**, 7857 (1991); 10.1063/1.460121

[Molecular beam studies of the photodissociation of benzene at 193 and 248 nm](#)

J. Chem. Phys. **92**, 4222 (1990); 10.1063/1.457780

[Stateresolved photofragmentation dynamics of Fe\(CO\)₅ at 193, 248, 266, and 351 nm](#)

J. Chem. Phys. **88**, 6658 (1988); 10.1063/1.454406

[Photofragmentation dynamics of acetone of 193 nm: State distributions of the CH₃ and CO fragments by time and wavelengthresolved infrared emission](#)

J. Chem. Phys. **85**, 817 (1986); 10.1063/1.451289



State resolved photofragmentation of Ni(CO)₄ at 193, 248, and 308 nm: A detailed study of the photodissociation dynamics

F. J. Schlenker, F. Bouchard, I. M. Waller,^{a)} and J. W. Hepburn^{b)}

Centre for Molecular Beams and Laser Chemistry, Department of Chemistry, University of Waterloo, Waterloo, Ontario, Canada N2L 3G1

(Received 17 May 1990; accepted 1 June 1990)

The vibrational, rotational, and translational energy distributions for the CO photofragments from the 193, 248, and 308 nm photolysis of Ni(CO)₄ in a supersonic molecular beam have been determined by vacuum ultraviolet laser-induced fluorescence. The measured product energy distributions appeared to be statistical, with equilibrium between the degrees of freedom investigated. The distributions were significantly colder than those calculated with a microcanonical statistical model using published bond energies. To model the measured distributions, it was necessary to postulate that the unsaturated nickel carbonyl products are formed in a stable electronically excited state. By using an excited state energy consistent with published fluorescence experiments, excellent agreement was obtained between the measured distributions and those calculated using a microcanonical statistical model. These results indicate that for 193 nm photolysis, essentially all of the Ni(CO)_n products are electronically excited, with about 2.8 eV of electronic excitation. The Ni(CO)_n products from 248 nm photolysis are formed in both the ground and excited states, with a 3:1 branching ratio. The data taken at 308 nm also indicate the presence of both channels, with the excited state channel still important. These results are consistent with predictions of earlier *ab initio* work, although the detailed mechanism is somewhat different. This earlier work is discussed in light of the present results.

INTRODUCTION

In recent work on the photofragmentation dynamics of a range of organometallics, the dynamics have been shown to be statistical, with sequential loss of ligands following excitation. In most cases where product energy distributions have been determined, these have been accurately modeled by statistical calculations, assuming complete randomization of the available energy before every dissociation step.¹⁻⁴ Metal carbonyl compounds have been emphasized in this detailed work, as their simple structure allows for accurate statistical calculations using known bond energies and vibrational frequencies.

One of the most thoroughly studied systems has been iron pentacarbonyl, where the detailed mechanism has been conclusively established by chemical trapping studies,⁵ transient infrared absorption,⁶⁻⁸ photofragment translational spectroscopy,^{3,9} and laser-induced fluorescence detection of the CO product.^{1,2} This last work used vacuum ultraviolet laser-induced fluorescence (VUV LIF) to determine the vibrational, rotational, and translational energy distributions for the CO photofragments formed over a range of excitation wavelengths from photolysis of Fe(CO)₅ in a supersonic beam. For all of the wavelengths studied, the measured energy distributions were reproduced by microcanonical calculations which used unadjusted literature values for bond energies and vibrational frequencies, and assumed sequential CO elimination preceded by complete energy randomization.

One of the only other metal carbonyl compounds for which all of the bond energies and vibrational frequencies have been measured is Ni(CO)₄. Nickel carbonyl has a photochemistry typical of the metal carbonyls, showing a loss of a single carbonyl group in solution, with a fairly low quantum yield, but with more extensive fragmentation in the gas phase.¹⁰ The electronic structure of Ni(CO)₄ and the possible photofragments are known, and the ground electronic states for the possible Ni(CO)_n fragments are closed shell singlet states, which is not the case for the photofragments from Fe(CO)₅. A possible contrast between the photochemistry of Ni(CO)₄ and Fe(CO)₅ arising from the different electronic structures was suggested by Veillard and coworkers,¹¹ in a paper reporting a theoretical study of the dissociation of Fe(CO)₅. This work was an elaboration of the idea, expressed in an earlier publication,¹² that state correlation diagrams could be used to predict the photochemistry of organometallic compounds. In the case of Fe(CO)₅, the ground state of Fe(CO)₄ + CO is correlated with an excited state in Fe(CO)₅, which implies ground state photoproducts, and a slow recombination rate for Fe(CO)₄ + CO. These had been observed experimentally, and the qualitative explanation was supported by the more detailed *ab initio* work.¹¹ For Ni(CO)₄, the ground state of Ni(CO)₃ + CO correlates with the ground state of Ni(CO)₄, while the excited state of Ni(CO)₄ correlates with the excited state of Ni(CO)₃ + CO, from which one might expect excited state photoproducts.

The observation of fluorescence resulting from the ultraviolet photodissociation of gas phase Ni(CO)₄¹³ was interpreted as evidence for the formation of excited state pho-

^{a)} Present address: Department of Chemistry, University of California, Berkeley, CA 94720.

^{b)} Alfred P. Sloan Foundation Fellow, 1988-90.

tofragments. A detailed *ab initio* study¹⁴ supported this, and found that the excited state of Ni(CO)₄ dissociated smoothly to excited state Ni(CO)₃ products. These results are especially intriguing in that the observed fluorescence had a long lifetime,¹³ and showed vibrational structure,¹⁵ indicating that the excited state products were stable with respect to dissociation.

In this paper, state resolved experiments on the 193, 248, and 308 nm photolysis of Ni(CO)₄ are reported. These measurements, carried out under collision free molecular beam conditions, determined the vibrational, rotational and translational energy distributions of the CO fragments, as was done previously for Fe(CO)₅.^{1,2} These results have been interpreted with the statistical model developed for Fe(CO)₅,² using published bond energies and vibrational frequencies. This work shows that the excited state channel is dominant at short wavelengths, even though the energy release in both the excited state and ground state channels is otherwise completely statistical. The results reported in this paper show that for 193 nm photolysis essentially all of the Ni(CO)_n fragments are formed in electronically excited states, while at 248 and 308 nm, the products are a mixture of ground and excited state Ni(CO)_n.

EXPERIMENT

The experimental method used in this study has been described in detail in previous publications.^{2,16,17} Briefly, a supersonic jet containing 2% Ni(CO)₄ in He was formed by expansion from a pulsed source with a 0.5 mm diameter nozzle. The Ni(CO)₄ (Strem Chemicals) was purified by vacuum distillation, and several freeze-pump-thaw cycles, and held in a cylinder kept at $-23\text{ }^{\circ}\text{C}$ by an ethylene glycol/water slush bath. He gas at about 1 atm pressure was bubbled through the Ni(CO)₄, and the resulting gas mixture fed into the source. The loosely focussed output of an ArF (193 nm), KrF (248 nm), or XeCl (308 nm) excimer laser (Lumonics HyperEX 400) intersected the supersonic jet at right angles 3 cm from the nozzle. The excimer laser was attenuated to pulse energies on the order of 1 mJ/pulse by a solution filter, and the power held constant by microprocessor control of the electrode voltage. To insure that the photolysis was strictly a single photon process, the power dependence of the CO signal was measured, and was found to be linear in photolysis pulse energy over the range 0 to 3 mJ/pulse for 193 nm, 0 to 4 mJ/pulse at 248 nm, and 0 to 20 mJ/pulse at 308 nm. The pulse energies used were well within the linear range. Under the loose focusing conditions used, the energy fluences were on the order of 10 to 20 mJ/cm² for the 15 ns pulses of 193 and 248 nm light.

For the 308 nm photolysis, the Ni(CO)₄ absorption cross section is very small, so it was necessary to use a higher photolysis laser power, and Ni(CO)₄ concentration in the beam. For these experiments, the Ni(CO)₄ reservoir was maintained at 0 °C, which resulted in a 10% concentration in the jet. The photolysis laser pulse energy was between 5 and 10 mJ/pulse, and the power dependence of the signal was linear over this entire range and up to 20 mJ/pulse.

The CO products of the photodissociation were detected by vacuum ultraviolet laser-induced fluorescence (VUV

LIF), using tunable VUV generated by four wave sum mixing in Mg vapor.¹⁷ The probe laser intersected the photolysis volume at right angles with the molecular beam and excimer laser, and was delayed about 500 ns after the excimer pulse. A variety of CO bands were excited to probe the CO($v=0,1,2$) products, and the LIF signal was collected by a LiF lens and detected by a solar blind PMT (EMR 542G-08-17). The fluorescence intensity was normalized by the measured VUV power, and the resulting LIF spectrum was analyzed to get the rotational distribution of the CO products in a given vibrational state. Vibrational distributions were determined by measuring LIF spectra for several different bands, and correcting the relative band intensities by the appropriate Franck–Condon factors.² Translational energy of the CO products was measured by Doppler spectroscopy on selected lines in the (2,0) and (3,0) bands of the LIF spectrum.

RESULTS AND ANALYSIS

CO (ν, J) distributions

For both 193 nm and 248 nm photolysis, spectra of the (2,0), (3,0), (0,0), (0,1) and (2,2) bands of the $A\ ^1\Pi \leftarrow X\ ^1\Sigma^+$ system were measured, while for 308 nm, only the (2,0) band was measured. For unperturbed rotational lines within those bands, the lines were numerically integrated, and divided by the VUV power and the appropriate Honl–London factor to give the relative population of the corresponding J state. Lines from the P , Q , and R branches were analyzed for several spectra, and the resulting relative populations for a given (ν, J) state were averaged together. To present this data, Boltzmann plots of $P_{\text{rel}}(\nu, J)$ as a function of rotational energy were made for the different bands probed. These plots are shown in Figs. 1, 2, and 3. The error bars shown are based on the scatter observed for a given (ν, J) level, and are not accurate reflections of the true uncertainty for J states where there was not much data ($\nu=1,2$, and very high J in $\nu=0$). A more accurate assessment of the uncertainty can be obtained by the scatter of the measured points around the calculated curves, which will be described in the next section. For very low J , data was not obtained because of spectral congestion, and a small contamination of the Ni(CO)₄ beam with CO, which was cooled to low J by the supersonic expansion.

For 193 and 248 nm photolysis, the relative populations of CO in $\nu=0,1$, and 2 were determined by comparing the relative intensities of several pairs of nearby bands in the CO excitation spectrum. For determining the $\nu=0:\nu=1$ ratio, the following pairs of bands were compared: (3,0) and (4,1), (2,0) and (3,1), and (0,0) and (1,1). The ratio of $\nu=1:\nu=2$ was measured by comparing the (0,1) and (2,2) bands. To make these comparisons, portions of the pair of bands being compared were scanned several times. Using the previously measured rotational distributions, and calculated Franck–Condon factors for the bands, the relative intensities of the rotational lines measured were converted into relative populations for the vibrational states detected. The results of these measurements are given in Fig. 4, along with the statistical calculation (*vide infra*).

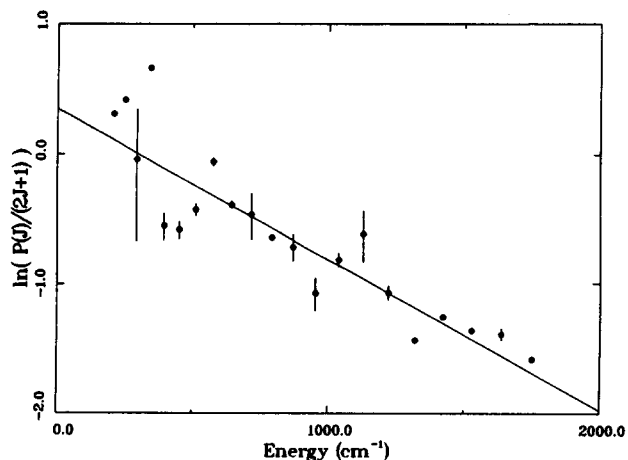
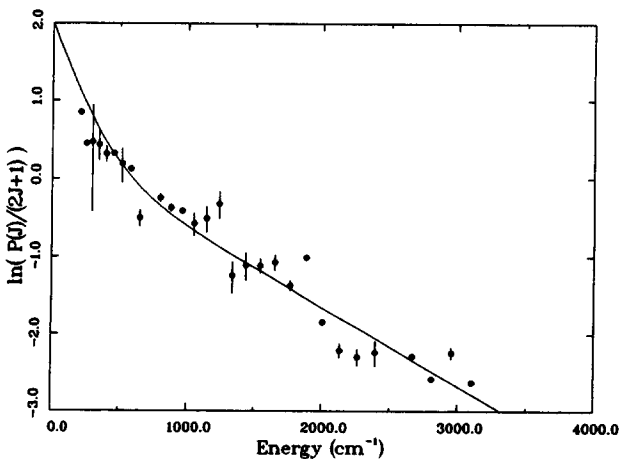
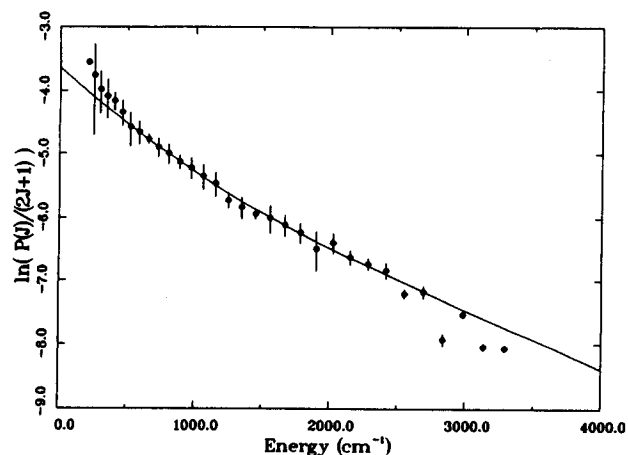


FIG. 1. Boltzmann plots of the measured relative populations for the CO($v = 0, 1,$ and 2) products from the 193 nm photolysis of Ni(CO)₄ (top, middle, and bottom, respectively). The solid line is the result of the statistical calculation described in the text.

Doppler profiles

A sample Doppler profile for an isolated rotational line in the (2,0) band of CO is given in Fig. 5. Several such lines were measured for CO($v = 0$) products from both 193 nm and 248 nm photolysis. The laser linewidth was determined by measuring the Doppler profiles of CO cooled in the jet, and this measured line profile was used to analyze the prod-

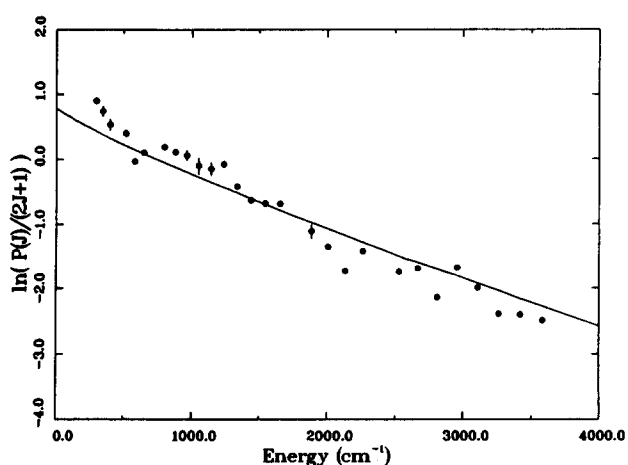
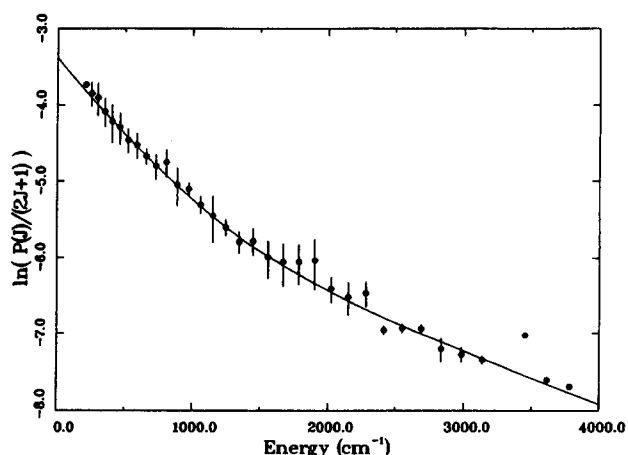


FIG. 2. Boltzmann plots of the measured relative populations for the CO($v = 0$ and 1) products from the 248 nm photolysis of Ni(CO)₄ (top and bottom, respectively). The solid line is the result of the statistical calculation described in the text.

uct Doppler profiles. Since a near-Boltzmann distribution of product energies was observed for both rotational and vibrational energy, a Gaussian Doppler profile was used to fit the measured data. To compare with the data, this Gaussian was convoluted with the measured line profile, and the solid line

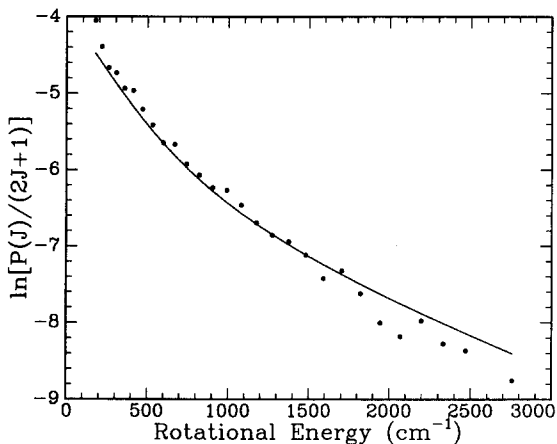


FIG. 3. Boltzmann plot for the measured rotational distribution for the CO($v = 0$) products from the 308 nm photolysis of Ni(CO)₄. The solid line is the result of the statistical calculation described in the text.

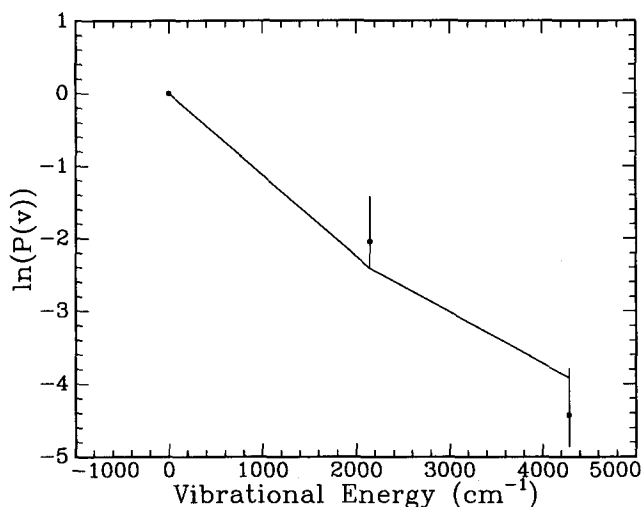
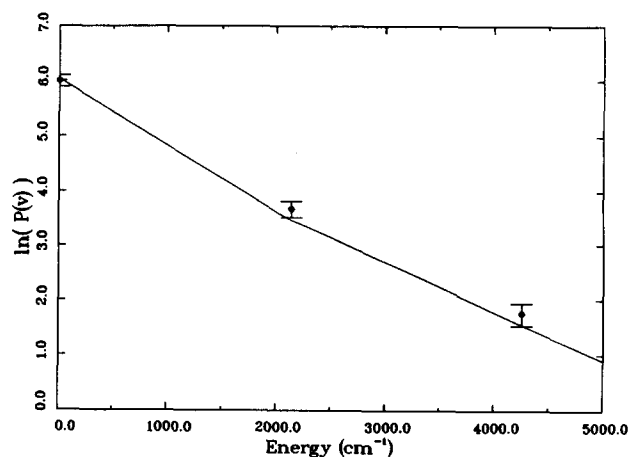


FIG. 4. Measured CO product vibrational distributions for 193 and 248 nm photolysis (top and bottom, respectively). Solid lines result from the statistical calculation described in the text.

drawn through the data in Fig. 5 is the result of such a convolution. For the 248 nm photolysis, the Gaussian which fit the data corresponded to a translational temperature of 1800 ± 300 K, while for 193 nm, the translational temperature was found to be 1500 ± 350 K.

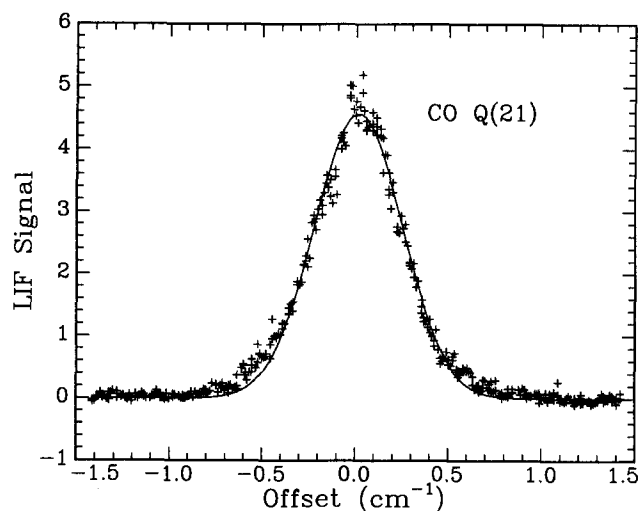


FIG. 5. Doppler profile for the CO($v=0$, $J=21$) product [$Q(21)$ line] from the 248 nm photolysis of Ni(CO)₄.

DISCUSSION

Statistical calculation

The data presented in Figs. 1 to 5 all show near Boltzmann energy distributions for the products of both 193 nm, 248 nm, and 308 nm photolysis of Ni(CO)₄. Furthermore, the “temperatures” that one would determine from the Boltzmann plots and Doppler line shapes are roughly the same for translation, rotation, and vibration in the CO products. This strongly suggests some sort of statistical partitioning of energy in the products, so statistical calculations of the product energy distributions were carried out. As the method of calculation has been described in great detail in a previous paper,² only an outline of the method will be given here.

The basis for this calculation was the assumption that the photofragmentation was a multistep process. The energy of the starting jet-cooled Ni(CO)₄ was assumed to be negligible, so the total energy available for the unimolecular reaction was given by the photon energy (6.42 eV for 193 nm, 5.00 eV for 248 nm, 4.02 eV for 308 nm). Before the first fragmentation step occurred, this photon energy was randomized in all the degrees of freedom of the Ni(CO)₄, resulting in a statistical distribution of energy for the products from the first dissociation step, Ni(CO)₃ + CO.

To calculate this energy distribution, attention was focused on the CO fragment, on which all the measurements were made. For a given CO(v, J) product, the available energy is defined as: $E_{avl} = h\nu - D_0 - E_{CO(v, J)}$, and the probability of forming that product is proportional to the total degeneracy of the Ni(CO)₃ + CO system at that energy. The Whitten–Rabinovitch approximation was used to calculate the state sum, because of the large density of states in this system, and separate calculations were carried out for each CO(v, J) state. It was found that the resulting microcanonical distributions were near thermal, so a temperature was used to describe them. This product temperature was then used to calculate a classical internal energy distribution for the Ni(CO)₃ fragment, and from this the fraction of Ni(CO)₃ with internal energies above the next dissociation threshold was calculated. The average energy of those dissociating Ni(CO)₃ molecules was calculated, and used as the total energy of the system for the next step in the dissociation which produced Ni(CO)₂ + CO. For these products, the same calculation was carried out, and this stepwise process was repeated until the Ni(CO)_{*n*} fragments did not have enough internal energy to dissociate. The overall CO product energy distribution was then determined by adding together the distributions for all the steps in the dissociation, weighted by the amount of CO produced in each step, and these calculated distributions were then compared with the data.

To calculate more accurate vibrational energy distributions for the Ni(CO)_{*n*} fragments, the SSE method was used.^{3,24} These calculations give exactly the same CO energy distribution for the first step in the dissociation, but provide a more accurate picture of the vibrational energy distribution in the Ni(CO)₃ fragment than a simple thermal distribution. This can affect the subsequent steps in the dissocia-

TABLE I. Ni(CO)_n-CO bond energies.

Bond energies for Ni(CO) _n (from Ref. 18, see discussion).	
Ni(CO) ₃ -CO	1.1 ± 0.1 eV
Ni(CO) ₂ -CO	0.8 ± 0.4 eV
Ni(CO)-CO	2.3 ± 0.7 eV
Ni-CO	1.3 ± 0.7 eV

tion, and perhaps give rise to different CO energy distributions. In the present case, it turns out that there is little difference between the results of the two different calculations, since the Ni(CO)₃ vibrational distribution is nearly thermal, and most of the Ni(CO)₄ molecules excited do not proceed beyond loss of two CO's, because of the high bond dissociation energy for the NiCO-CO bond. Because of this, distributions were calculated using the simpler method that we have applied previously to Fe(CO)₅.²

To carry out these calculations, one needs to have values for the Ni(CO)_n-CO bond energies for all the steps, and vibrational frequencies for the various Ni(CO)_n fragments. These have all been measured in previous work, so literature values were used. The bond energies used are given in Table I, and these are based on the numbers published by Stevens *et al.*¹⁸ These values, measured by negative ion photoelectron spectroscopy, had reasonably large error bars, and gave a total of 5.3 eV for the energy to go from Ni(CO)₄ to Ni + 4CO, in disagreement with the thermodynamic total of 6.10 ± 0.1 eV measured by Cotton and coworkers.¹⁹ For the first bond, Ni(CO)₃-CO, the 1.1 ± 0.1 eV bond energy determined by Stevens *et al.*¹⁸ was in good agreement with the results of a kinetics measurement of 0.96 eV,²⁰ and so 1.1 eV was used. The second bond energy of 0.6 ± 0.4 eV seemed too weak, and in light of the disagreement in the total bond energies, a 0.8 eV bond energy was used in the statistical calculations, in keeping with the pattern of a lower second bond energy. As there was no other data for the third and fourth bond energies, the values of Stevens *et al.*¹⁸ were used. These bond energies are very reasonable, in light of the total heat of formation of Ni(CO)₄, and the low values for the first two bonds. The vibrational frequencies used are presented in Table II, and these were all taken from the literature.^{18,21-23} The results of the statistical calculation are not strongly dependent on these frequencies, as long as reasonable values are used.

193 nm photolysis, excited state channel

In previous work on Fe(CO)₅, calculations exactly like those described above reproduced experimentally determined product energy distributions very well, at all wavelengths investigated.^{2,3} This was not at all the case for Ni(CO)₄ dissociated at 193 nm, where calculations using the parameters given in Tables I and II resulted in much more internal energy in the CO products than was measured. As an example of this, Fig. 6 shows the measured rotational distribution for the CO(*v* = 0) products from the 193 nm photolysis, along with the calculated rotational distribution. Since the only possible fragmentation channels are CO elimination, and all CO degrees of freedom are measured, these

TABLE II. Ni(CO)_n vibrational frequencies. Vibrational frequencies for Ni(CO)_n fragments. Unless otherwise indicated, values are from Ref. 23.

Molecule	Vibration	Frequency (cm ⁻¹)	Degeneracy
Ni(CO) ₃	C-O sym stretch	2100 ^a	1
	Ni-C sym stretch	337	1
	C-O assym stretch	2017 ^b	2
	Ni-C-O in plane bend	503	2
	Ni-C assym stretch	457 ^b	2
	C-Ni-C in plane bend	63	2
	Ni-C-O in plane bend	346	1
	Ni-C-O out of plane bend	421	1
	C-Ni-C out of plane bend	75	1
	Ni-C-O out of plane bend	296	2
Ni(CO) ₂	C-O sym stretch	2100 ^a	1
	Ni-C sym stretch	403	1
	C-O assym stretch	1967 ^b	1
	Ni-C assym stretch	516 ^b	1
	Ni-C-O assym bend	379	2
	Ni-C-O sym bend	448	2
C-Ni-C bend	82	2	
NiCO	C-O stretch	1996 ^b	1
	Ni-C stretch	607	1
	Ni-C-O bend	460	2

^a From Ref. 18.

^b From Ref. 22.

results indicate that some of the expected available energy is not released in the dissociation, but contained in an internal degree of freedom not available for fragmentation. Recalling that we have determined all of the energy distributions except the internal energy of the Ni(CO)_n fragments, the "hidden" energy must rest in these products.

The degree of freedom that would seem most likely, vibrations in the Ni(CO)_n products, does not explain these experimental results. Since the calculation assuming complete energy randomization resulted in CO products that were much "hotter" than those observed, one would have to postulate that the available energy is not randomized before

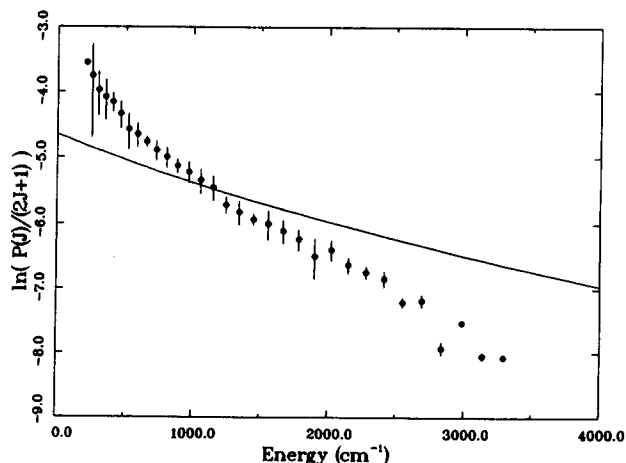


FIG. 6. Rotational distribution for the CO(*v* = 0) products from the 193 nm photolysis of Ni(CO)₄ (points), together with the result of a statistical calculation based on ground state Ni(CO)_n products (solid line).

TABLE III. CO temperatures and weighing factors from the microcanonical statistical calculation.

Photolysis wavelength	Channel	Vibrational level	Temp. #1(K)	Temp. #2(K)
193 nm	excited	$v = 0$	1600(0.50)	620(0.50)
	excited	$v = 1$	1440(0.56)	260(0.44)
	excited	$v = 2$	1260(1.0)	...
248 nm	excited(.75)	$v = 0$	600(.600)	...
	ground(.25)	$v = 0$	2600(.200)	1780(.200)
	excited(.05)	$v = 1$	355(0.02)	...
	ground(.95)	$v = 1$	2420(0.49)	1320(0.49)
	ground	$v = 2$	2250(.50)	850(0.50)
308 nm	ground	$v = 0$	1957(0.28)	1007(0.28)
	excited	$v = 0$	280(0.43)	...

dissociation, but stays more in the Ni(CO)_n fragment, resulting in a “colder” CO product. The problem now is that much more energy is left in the Ni(CO)₃ product, with fewer degrees of freedom available. Using a simple thermal model,¹ one finds that if the initial CO products have their internal and translational energies fixed at 1000 K, the “temperature” of the resulting Ni(CO)_n fragments increases as the dissociation proceeds, ending with a NiCO fragment at an internal temperature greater than 5000 K. Since such a hot molecule will dissociate, the result will be a very hot CO product, which was not observed.

In light of the previous observations of fluorescing products from ultraviolet photolysis of Ni(CO)₄,^{13,15} and the *ab initio* analysis which predicted the formation of such products,¹⁴ it seemed more reasonable to postulate the formation of electronically excited Ni(CO)_n photofragments, which can store energy in a form not available to the fragmentation energy release. If it is assumed that the electronic excitation in these products can only be lost by fluorescence, this energy is thus not available for dissociation. This excitation can be accounted for in the statistical model by adding it to the bond dissociation energy used in the calculation, to get an overall heat of formation for the excited fragments. At 193 nm, the large photon energy gives rise to excited state Ni(CO)₃ products with an internal energy greater than the Ni(CO)₂-CO bond energy (0.8 eV). To treat this case, the electronic excitation in the Ni(CO)₃ was assumed adiabatic, and retained by the Ni(CO)₂ product, resulting in the energy remaining “hidden” from the photodissociation product vibrational, rotational, and translational degrees of freedom.

To treat this excited state channel, it was necessary to assume an energy for the Ni(CO)₃ excited state formed in the dissociation. For this, the dispersed fluorescence results^{13,15} served as a guide. In both studies, the high energy end of the fluorescence spectrum was at 2.4 eV, indicating that the excited state was at an energy of about 2.4 eV. The *ab initio* study¹⁴ indicated a large geometry change between ground and excited state Ni(CO)₃, so essentially no (0,0) band fluorescence would be expected. Since the photon energies used were not too far above the threshold for creating excited state Ni(CO)₃, the Ni(CO)₃^{*} would not be highly vibrationally excited, meaning the high energy limit of the

fluorescence spectrum provides a lower limit to the energy of the excited state.

In our calculations the best agreement between the observed and statistical product energy distributions was found by using an excited state energy of 2.8 eV, in good agreement with the 2.4 eV lower limit observed in fluorescence. Given the uncertainty in the bond energies, and the approximate nature of the statistical model, this agreement in energy is quite good. It must be stressed that we are not claiming to provide a quantitative measure of the excited state energy, but we do expect our value to be close to the true value.

To model the 193 nm data, it was assumed that all the Ni(CO)_n products were electronically excited. By making this assumption, and using a first bond energy of 1.1 + 2.8 eV, the CO product temperatures given in Table III were calculated. Since two CO products were formed per 193 nm photon, the two distributions were added together to compare to the data. The solid lines given in Figs. 1 and 4 are the result of this, and the agreement between calculation and experiment can be seen to be excellent. The dispersion in the data and the uncertainty associated with the statistical model prevent a definitive statement about the lack of ground state product, but it would appear certain that the majority of products formed at 193 nm are in electronically excited states.

This observation is quite striking, given the otherwise statistical nature of the dissociation. The detailed *ab initio* calculations of Rosch *et al.*¹⁴ found two excited states of Ni(CO)₄, the 2A₁ and 1E states, that were repulsive in the Ni-CO coordinate and were correlated with excited state Ni(CO)₃ products. If these states participate in the dissociation, then excited state products would be expected. However, if these repulsive states were populated directly, and the dynamics proceeded through a simple Ni(CO)₃-CO repulsion, one would not expect a statistical energy partitioning, but would expect more energy to be channeled into CO translation and rotation. From the calculated potentials, direct excitation of the 2A₁ and 1E states would have extremely unfavorable Franck-Condon factors for excitation at photon energies of 6.4 eV. Furthermore, there are very likely many more states involved in the excitation process, so the

excitation cannot be viewed in terms of a two state picture, with the upper state repulsive in the Ni(CO)₃-CO coordinate. A more likely mechanism is that the original excitation is to several "different" excited states, which are then coupled to the dissociative continuum in a way that the excitation energy is randomized into the nuclear degrees of freedom before the dissociation. The result is an RRKM like dissociation, but with excited state products as the outcome, meaning a much higher effective energy for the Ni(CO)₃-CO bond.

248 nm photolysis

The measured distributions for 248 nm photolysis also appeared statistical, as can be seen from Figs. 2 and 4. When the 248 and 193 nm data are compared, two definite observations can be made about the data. The first is that at 248 nm, the measured rotational distribution is more noticeably bimodal than at 193 nm, with a high temperature component at a similar temperature to the average observed at 193 nm. Secondly, while the $v = 0$ and $v = 1$ distributions were similar at 193 nm, for 248 nm, the $v = 1$ distribution has a much higher average temperature than $v = 0$, and in fact has a higher average temperature than the 193 nm $v = 0$ distribution. The smaller photon energy at 248 nm (5.0 vs 6.4 eV) should give rise to much colder products, if the same excited state products are formed. An explanation for these observations is that ground state Ni(CO)_n fragments are formed at 248 nm, along with the excited state products.

If this is the case, the large difference in the available energy for the two channels (3.9 eV for ground state vs 1.1 eV for excited state), will result in two very different energy distributions for the CO fragments, a hot one for those products in coincidence with ground state Ni(CO)₃ products, and a cold one for the CO from the excited state channel. These two different distributions were calculated using the statistical model, and then the relative amount of each distribution required was fitted to the data. The data was best reproduced by a branching ratio of 3:1 between the excited and ground state channels. In the ground state channel, the initially formed Ni(CO)₃ product also dissociated, resulting in a second CO product. For the excited state channel, the Ni(CO)₃* product was largely undissociated, so only one CO product was formed. The temperatures and weighing factors for the various CO products are given in Table III. The resulting calculated distributions, multiplied by the appropriate factors, were summed together to give the calculated distribution shown in Figs. 2 and 4.

Since there is little CO($v = 1$) formed in the excited state channel, vibrationally excited CO results almost entirely from the ground state channel, and thus the $v = 1$ rotational energy distribution reflects the ground state channel dynamics. This results in a hotter rotational distribution for CO($v = 1$), compared with CO($v = 0$). The results of the statistical calculation for the $v = 1$ CO products are given in Table III, and the calculated distribution shown in Fig. 2 is from the listed parameters.

308 nm photolysis

The data for 308 nm photolysis are not as extensive as for the other wavelengths, and not as reliable. However, some qualitative results can be derived from this data, based on the results for 193 and 248 nm. The rotational energy distribution for the CO($v = 0$) product is shown in Fig. 3, and once again, it appears statistical. Since the previous experiments in which fluorescing products were observed were carried out at photolysis wavelengths of 308 nm,¹³ 351 and 364 nm,¹⁵ excited Ni(CO)₃ products can be expected. What is not known is the quantum yield for these products, although Rosch *et al.*¹³ estimated 10%.

To reproduce the data shown in Fig. 3, the same statistical calculation that was carried out for the 248 nm was used, but a higher fraction of ground state products was assumed. The solid line through the measured data shown in Fig. 3 corresponds to a quantum yield of 60% for the excited state channel. This number should be regarded with some caution, as a higher concentration of Ni(CO)₄ in He was used in the beam than at 193 and 248 nm, because of the much smaller absorption cross section. This could have resulted in increased cluster formation, and a fraction of the observed CO could have resulted from photolysis of van der Waal's clusters, which could produce lower temperature products,^{25,26} and increase the apparent yield of the excited state channel. However, while we would not want to claim to have measured the excited state vs ground state branching ratio accurately at 308 nm, the data indicates that a large fraction of the products result from the excited state channel. As was found at 248 nm and 193 nm, the data was also reproduced very well by the statistical model, meaning the dynamics in both ground and excited channels are completely statistical.

OVERALL MECHANISM AND DYNAMICS

Several general comments can be made about the photodissociation dynamics of Ni(CO)₄. The overall mechanism is similar to that found previously for Fe(CO)₅, in that the loss of CO after photoexcitation occurs sequentially, with the available energy distributed statistically amongst the product degrees of freedom. This statistical partitioning of energy in the products indicates that the dissociation proceeds in an RRKM fashion, with internal relaxation within the excited Ni(CO)₄ occurring on a faster time scale than dissociation. This implies that the dissociation does not proceed simply through excitation of a single excited state surface that is repulsive in the Ni(CO)₃-CO coordinate, as suggested by *ab initio* work,¹⁴ but rather occurs through excitation of a "mixture" of strongly coupled excited states, which then are coupled less strongly to the continuum.

In Fe(CO)₅, the excitation wavelength only affected the dissociation dynamics by controlling the total energy available to the microcanonical ensemble at the beginning of the dissociation sequence. The dissociation mechanism was independent of the nature of the dissociating excited state prepared, and no evidence was found for significant yield of excited state fragments.² In Ni(CO)₄, while statistical behavior in nuclear degrees of freedom was found at all photolysis wavelengths studied, our data also showed significant

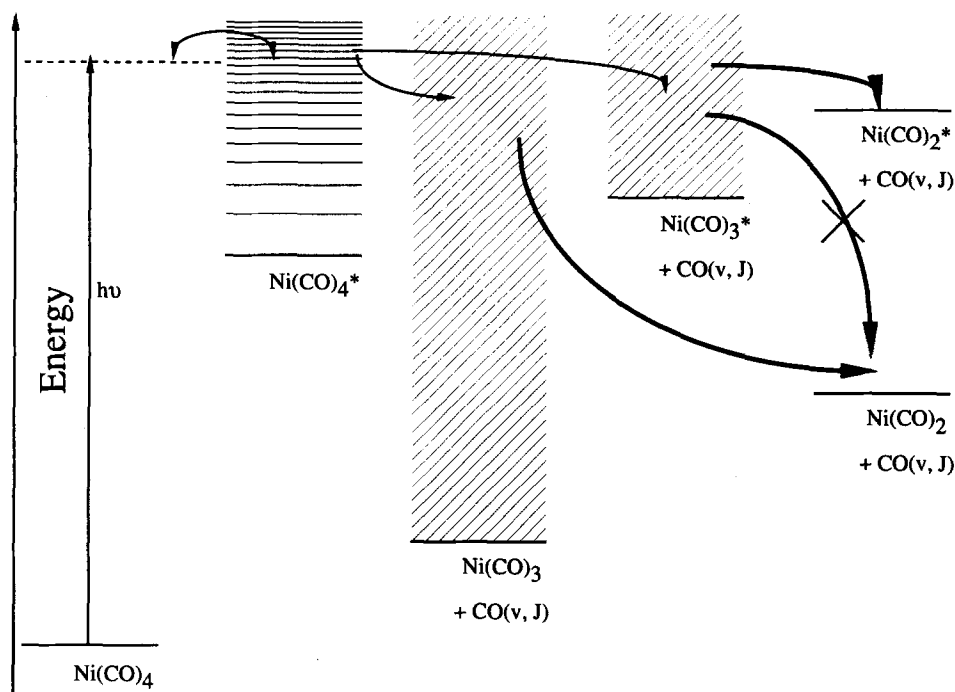


FIG. 7. Schematic diagram of Ni(CO)₄ photolysis mechanism.

wavelength dependent yield of excited state fragments. This contrast between Ni(CO)₄ and Fe(CO)₅ is indicative of an important difference between the dynamics of the two systems, which results from the difference in electronic structure.

As discussed above, the excited singlet states of Ni(CO)₄ are not correlated with ground state Ni(CO)₃ + CO, but with excited state Ni(CO)₃ + CO,¹¹ because of the correlation between ground state Ni(CO)₄ and ground state Ni(CO)₃ + CO. This simple picture, confirmed by *ab initio* calculations,¹⁴ is in contrast with Fe(CO)₅, where the ground state of Fe(CO)₄ is a triplet, and thus not correlated with ground state Fe(CO)₅,^{11,12} but with an excited state. The result is that in Fe(CO)₅, the relaxation occurs within the excited state manifold, and the coupling out is to the ground triplet state continuum, while in Ni(CO)₄, the coupling to the excited state continuum dominates for ultraviolet excitation.

In Ni(CO)₄, this indirect coupling with the excited state dissociation continuum is most important for short wavelength excitation, and it would appear that given sufficient vibrational energy the excited Ni(CO)₃ products formed dissociate adiabatically to give excited state Ni(CO)₂. Furthermore, the excited state fragments formed, either Ni(CO)₃ or Ni(CO)₂, are stable and do not predissociate. The branching ratio between the Ni(CO)₃ + CO excited and ground state channels was also found to vary with the photolysis wavelength. At 193 nm, the products were formed almost entirely on the excited state surface while at 248 nm, about 25% of the Ni(CO)₄ molecules dissociate on the ground state surface and at 308 nm the branching ratio is about one to one. One possible interpretation of this result is that the initially prepared Ni(CO)₄ excited state is coupled

simultaneously to the excited state and ground state dissociation channels, with a coupling that depends on the excitation wavelength. Within both of these channels, internal relaxation occurs faster than dissociation, so both ground and excited state products show a statistical energy partitioning. All of these features of the dissociation dynamics are shown schematically in Fig. 7.

Neither the present results, nor existing *ab initio* calculations reveal the detailed nature of the excited states or their couplings, but it would appear that the picture provided by *ab initio* work¹⁴ at least provides a basis for understanding the photodissociation of Ni(CO)₄. A tentative explanation for the wavelength dependence would be that at longer wavelengths, the presence of an internal conversion channel, which results in ground state products, becomes more noticeable. In Fe(CO)₅, there is evidence for the presence of excited state products at 193 nm from transient infrared absorption experiments.⁸ Although our previous work² showed that the excited state channel was minor at 193 nm, the existence of this channel could result again from correlations between the initially excited state in Fe(CO)₅ and the excited singlet state of the Fe(CO)₄ product, resulting in a coupling to this excited state continuum at higher photon energies.

The statistical model used for the CO internal energy distributions can also be used to calculate the distribution of Ni(CO)_n products at different wavelengths. These predicted photofragment distributions, the result of an SSE calculation using the bond energies given in Table I, are summarized in Table IV. As was found for Fe(CO)₅ dissociation, the distribution of fragments produced in the dissociation of Ni(CO)₄ appears nonstatistical, because of the distribution of Ni(CO)_n-CO bond energies in Ni(CO)_n. As an exam-

TABLE IV. Ni(CO)_n fragment distributions from Ni(CO)₄ photolysis.

Photolysis wavelength	Excited state		Ground state	
	Ni(CO) ₃	Ni(CO) ₂	Ni(CO) ₃	Ni(CO) ₂
193 nm	...	100%
248 nm	70%	5%	...	25%
308 nm	60%	40%
450 nm	100%

ple, the statistical calculation predicts that the products from the 193 nm dissociation will be essentially entirely excited state Ni(CO)₂. This result, similar to the finding that Fe(CO)₅ dissociation at 193 nm produces almost pure Fe(CO)₂ products,^{2,3} comes from the fact that the first and second bond energies in Ni(CO)₄ are weak, while the NiCO–CO bond is stronger, preventing further dissociation. Thus, an apparently nonstatistical fragmentation pattern⁵ is, in fact, predicted by a statistical model. Given an appropriate distribution of bond energies, this feature of the photodissociation dynamics in metal carbonyls can be exploited to provide chemically pure unsaturated metal carbonyls by photolysis for use in chemical dynamics studies.

It may also be possible to use these fragment distributions to provide “state selected” unsaturated nickel carbonyl fragments to study their subsequent reactions in detail. If the threshold for formation of excited state Ni(CO)₃ is at around 450 nm, photolysis at this wavelength will produce essentially pure Ni(CO)₂ in its ground state, since the photon energy is insufficient to produce excited state fragments. On the other hand, photolysis at 193 nm appears to produce Ni(CO)₂ in a stable excited state, with a long enough fluorescence lifetime that it may be possible to study its reactivity and properties.

Finally, while the present results provide very strong evidence for the production of stable excited state Ni(CO)_n products from Ni(CO)₄, the evidence is indirect in that we have not detected these fragments. More work needs to be done on the detection and characterization of these fragments, and the measurement of the quantum yield as a function of photolysis wavelength.

ACKNOWLEDGMENTS

This work was supported by NSERC and the donors of the Petroleum Research Fund, administered by the American Chemical Society. IMW and FB acknowledge the support of NSERC in the form of graduate scholarships. The authors would like to thank Doug Cyr for his assistance with some of the data collection.

- ¹I. M. Waller, H. F. Davis, and J. W. Hepburn, *J. Phys. Chem.* **91**, 506 (1987).
- ²I. M. Waller and J. W. Hepburn, *J. Chem. Phys.* **88**, 6658 (1988).
- ³U. Ray, S. L. Brandow, G. Bandukwalla, B. K. Venkataraman, Z. Zhang, and M. F. Vernon, *J. Chem. Phys.* **89**, 4092 (1988).
- ⁴S. Georgiou and C. A. Wight, *J. Chem. Phys.* **90**, 1694 (1989).
- ⁵J. T. Yardley, B. Gitlin, G. N. Nathanson, and A. M. Rosan, *J. Chem. Phys.* **74**, 370 (1981).
- ⁶A. J. Ouderkirk, P. Wermer, N. L. Schultz, and E. Weitz, *J. Am. Chem. Soc.* **105**, 3354 (1983).
- ⁷A. J. Ouderkirk and E. Weitz, *J. Chem. Phys.* **79**, 1089 (1983).
- ⁸T. A. Seder, A. J. Ouderkirk, and E. Weitz, *J. Chem. Phys.* **85**, 1977 (1986).
- ⁹B. K. Venkataraman, G. Bandukwalla, Z. Zhang, and M. F. Vernon, *J. Chem. Phys.* **90**, 5510 (1989).
- ¹⁰A. B. Callear, *Proc. R. Soc. London Ser. A* **265**, 71 (1971).
- ¹¹C. Daniel, M. Benard, A. Dedieu, R. Wiest, and A. Veillard, *J. Phys. Chem.* **88**, 4805 (1984).
- ¹²A. Veillard, *Nouv. J. Chim.* **5**, 599 (1981).
- ¹³N. Rosch, M. Kotzian, H. Jorg, H. Schroder, B. Rager, and S. Metev, *J. Am. Chem. Soc.* **108**, 4238 (1986).
- ¹⁴N. Rosch, H. Jorg, and M. Kotzian, *J. Chem. Phys.* **86**, 4038 (1987).
- ¹⁵D. M. Preston and J. I. Zink, *J. Phys. Chem.* **91**, 5003 (1987).
- ¹⁶I. M. Waller and J. W. Hepburn, *J. Chem. Phys.* **87**, 3261 (1987).
- ¹⁷D. J. Hart and J. W. Hepburn, *J. Chem. Phys.* **86**, 1733 (1987).
- ¹⁸A. E. Stevens, C. S. Feigerle, and W. C. Lineberger, *J. Am. Chem. Soc.* **104**, 5026 (1982).
- ¹⁹F. A. Cotton, A. K. Fischer, and G. Wilkinson, *J. Am. Chem. Soc.* **81**, 800 (1959).
- ²⁰J. P. Day, F. Basolo, and R. G. Pearson, *J. Am. Chem. Soc.* **90**, 6927 (1968).
- ²¹L. H. Jones, R. S. McDowell, and M. Goldblatt, *J. Chem. Phys.* **48**, 2663 (1968).
- ²²R. L. DeCock, *J. Inorg. Chem.* **6**, 1205 (1971).
- ²³P. Carsky and A. Dedieu, *Chem. Phys.* **103**, 265 (1986).
- ²⁴C. Wittig, I. Nadler, H. Reisler, M. Noble, J. Cantanzarite, and G. Radhakrishnan, *J. Chem. Phys.* **83**, 5581 (1985).
- ²⁵N. Sivakumar, I. Burak, W.-Y. Cheung, J. W. Hepburn, and P. L. Houston, *J. Phys. Chem.* **89**, 3609 (1985).
- ²⁶N. Sivakumar, G. E. Hall, P. L. Houston, J. W. Hepburn, and I. Burak, *J. Chem. Phys.* **88**, 3692 (1988).